

Open  
Access

## 2D Numerical Simulation of the Dichlorodifluoromethane Decomposition with O<sub>2</sub> and H<sub>2</sub> in Thermal Argon Plasma Reactor

Amine Brahim<sup>1,\*</sup>, Mohamed Announ<sup>1</sup>

<sup>1</sup> Materials and Environment Laboratory (LME), Faculty of Technology, University Yahia Fares of Medea, Algeria

### ARTICLE INFO

### ABSTRACT

#### Article history:

Received 30 March 2019

Received in revised form 20 May 2019

Accepted 2 June 2019

Available online 15 July 2019

A two dimensional analysis of the (CCl<sub>2</sub>F<sub>2</sub>) decomposition with O<sub>2</sub> and H<sub>2</sub> in DC thermal argon plasma reactor is carried out numerically using a CFD simulation. Firstly, a thermodynamic investigation of Ar/C/Cl/F/O/H system is conducted at a temperature range between 300K and 6000K in order to determine the main species and chemical reactions resulting from the decomposition of CCl<sub>2</sub>F<sub>2</sub>. Secondly, a two dimensional study is done numerically using the Fluent software with the turbulence model (k-ε) to solve the partial differential equations describing the mass, momentum and energy conservations which are all combined with the chemical kinetics of 17 species and 21 reactions obtained through the previous investigation. The results show that the CCl<sub>2</sub>F<sub>2</sub> is completely destroyed after breaking down into CO, CO<sub>2</sub>, HCl, HF and H<sub>2</sub>O at the outlet of the plasma reactor. Moreover, the addition of hydrogen in stoichiometric ratio is sufficiently enough to eliminate the chlorine, fluorine and hydroxyl radicals which make the whole process much less detrimental to the environment.

#### Keywords:

Thermal plasma; CCl<sub>2</sub>F<sub>2</sub>; FLUENT; Kinetic; decomposition; turbulence model (k - ε)

Copyright © 2019 PENERBIT AKADEMIA BARU - All rights reserved

## 1. Introduction

The dichlorodifluoromethane (CCl<sub>2</sub>F<sub>2</sub>), also known as CFC-12, had been long used as a safe refrigerant in refrigeration and air-conditioning as well as a propellant in aerosol sprays until 1974 when new research revealed that CFCs are the leading cause of the ozone layer depletion. Furthermore, it has recently been found that CFCs are also significantly responsible for worsening the global warming because they trap heat more than the conventional greenhouse gases [1].

The Montreal Protocol in 1987 as well as its 1997 revision in Kyoto called for the necessity to bring their use to an end by 2010, and since then, many scientists have been interested in the decomposition of the CFCs that are both in use and stock [2-3].

Many processes are used for the breakdown of these gases and one of them is done through thermal plasma [4-9] which seems to be highly effective in the total destruction of CFC molecules

\*Corresponding author.

E-mail address: [ami\\_brahimi@yahoo.fr](mailto:ami_brahimi@yahoo.fr) (Amine Brahim)

because of the high temperature of plasma. Moreover, the operating mechanism of thermal plasma, generated by DC arc discharge, is simpler and easier to handle in comparison with other processes [10-12].

However, the chemicals obtained from the CFCs decomposition such as the chlorine, fluorine and hydroxyl radicals can also be damaging to the environment and must therefore be completely eliminated. In order to achieve this purpose, the CFCs decomposition by using the thermal plasma process has to be well understood because it is a complex phenomenon which depends on the thermodynamics, the chemical kinetics, and the heat transfer as well as the fluid dynamics including the chamber reactor and the operating conditions. It is worth noting that the financial cost of conducting a practical experiment could be extremely high due to the difficulty in making quantitative analyses of all species in the plasma reactor. Until now, one dimensional model (1D) of the  $\text{CCl}_2\text{F}_2$  decomposition with  $\text{O}_2$  and  $\text{H}_2$  for laminar flow in argon thermal plasma tubular reactor has been investigated numerically by [13].

The conservation equations of energy and mass including the relation between enthalpy and reaction rate for all species were applied in each control volume. The result of this model indicates that the use of  $\text{H}_2$  in excess is effective in reducing the amount of  $\text{Cl}_2$ . However, this model doesn't properly simulate the process of  $\text{CCl}_2\text{F}_2$  decomposition because it does not take into consideration the thermal and hydrodynamic phenomena that occur in the reactor such as the multidimensional fluid flow and the variation in temperature and velocity in radial direction, as well as the turbulence. Therefore, this model seems to be inadequate to obtain accurate results. Thus, a CFD analysis is a powerful computing tool used in various practical conditions and can provide us with a clear image of all the species resulting from the decomposition of the  $\text{CCl}_2\text{F}_2$  along the reactor which may not be easily collected and measured experimentally.

In this work, a 2D analysis of  $\text{CCl}_2\text{F}_2$  decomposition with  $\text{O}_2$  and  $\text{H}_2$  in the thermal argon plasma reactor is numerically carried out using the FLUENT software. A set of coupled partial differential equations of fluid dynamics is combined with the chemical kinetics model to be numerically solved using the control volume method suggested by [14] to determine the concentration of all chemical species resulting from the decomposition of  $\text{CCl}_2\text{F}_2$ . In this study 17 species and 21 chemical reactions, which are all previously determined by the thermodynamic investigation of Ar/C/Cl/F/O/H system, are taken into consideration to obtain reliable results and avoid numerical instabilities in the computation.

## 2. Methodology

### 2.1 Thermodynamic Investigations

The thermodynamic equilibrium calculation of the decomposition of CFC-12 in the thermal argon plasma at a temperature range from 298K to 6000K and under atmospheric pressure is carried out with the gas system Ar/C/Cl/F/O/H which is itself a mixture of gases consisting of 0.04 moles of CFC-12, 0.04 mole of  $\text{O}_2$ , 0.08 mole of  $\text{H}_2$  and 0.8 mole of Ar. Based on the minimization of the Gibbs free energy theory [4,15], the calculation is performed by the HSC Chemistry software. 44 chemical species (molecules, radicals), whose Gibbs (free) energy data are available, are taken into consideration in the computation when calculating (Table 1).

**Table 1**  
 Considered chemical species as possible products of thermal plasma destruction of CFCs

|                                     |                     |                      |                     |                     |
|-------------------------------------|---------------------|----------------------|---------------------|---------------------|
| Ar(g)                               | CF(g)               | CH <sub>4</sub> (g)  | H <sub>2</sub> (g)  | HCO(g)              |
| C(g)                                | CF <sub>2</sub> (g) | C <sub>2</sub> H(g)  | Cl(g)               | HCl(g)              |
| C <sub>2</sub> CF(g)                | CF <sub>3</sub> (g) | CO(g)                | Cl <sub>2</sub> (g) | HClO(g)             |
| CCl(g)                              | CF <sub>4</sub> (g) | CO <sub>2</sub> (g)  | ClF(g)              | HF(g)               |
| C <sub>2</sub> Cl(g)                | C <sub>2</sub> F(g) | COCl(g)              | ClO(g)              | HO(g)               |
| CClF <sub>3</sub> (g)               | CH(g)               | COClF(g)             | F(g)                | HO <sub>2</sub> (g) |
| CCl <sub>2</sub> F <sub>2</sub> (g) | CH <sub>2</sub> (g) | COF(g)               | F <sub>2</sub> (g)  | H <sub>2</sub> O(g) |
| CCl <sub>3</sub> F(g)               | CH <sub>3</sub> (g) | COF <sub>2</sub> (g) | H(g)                | O(g)                |
| O <sub>2</sub> (g)                  | OH(g)               | C(s)                 |                     |                     |

The equilibrium concentration of chemical species as function of temperature is illustrated in Figure 1. The calculated concentration shows the absence of any trace of CFC-12 as a result of being completely destroyed. H<sub>2</sub>O are observed at about 3000K. HF, HCl, CO<sub>2</sub> and CO are the dominating species in the mixture of gas below 2000K. At T>2000K fluorine, chlorine in the atomic form exist. From this investigation it can also be noticed that from among 44 chemical species, there are only 17 species dominating and the rest are insignificant.

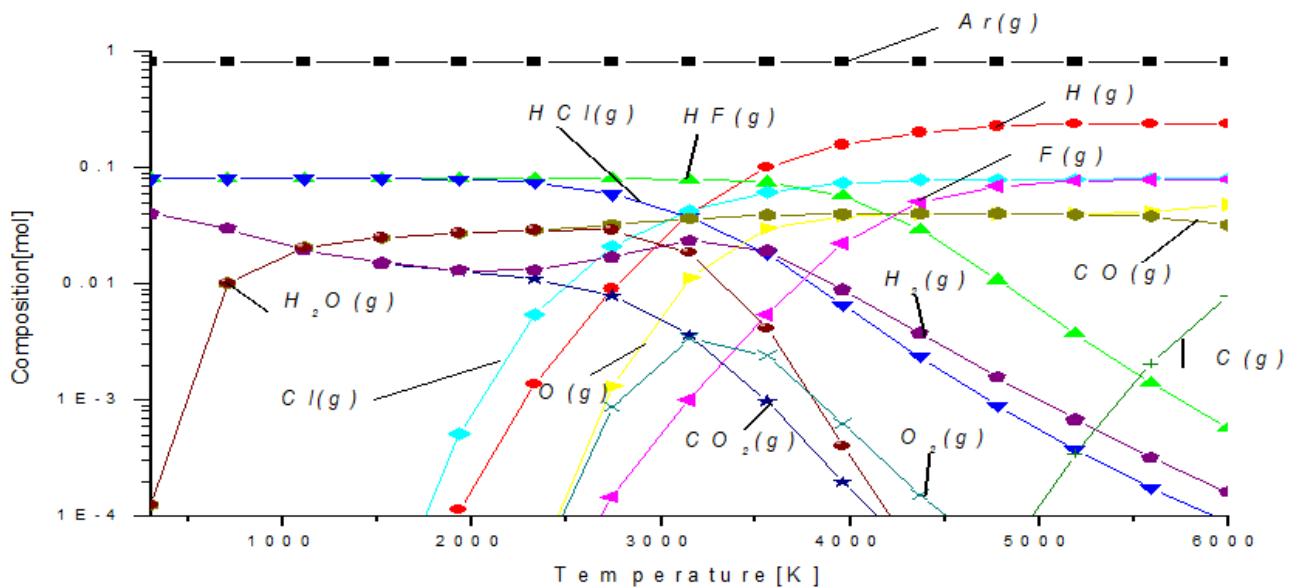


**Fig. 1.** Equilibrium composition in Ar/C/Cl/F/O/H gas system, as a function of temperature; Ar/CCl<sub>2</sub>F<sub>2</sub>/O<sub>2</sub>/H<sub>2</sub>: 0.8/0.04/0.04/0.08 p=1 bar

## 2.2 Problem Description

In this study a D.C. plasma torch is used to generate thermal argon plasma jet which flows from the nozzle into the reactor chamber as shown in Figure 2. The mixture of reactant gases that consists of CFC-12, O<sub>2</sub> and H<sub>2</sub> is injected downward through a tube between the outlet of argon plasma jet from the torch and the inlet of the reactor. The working conditions of the described process, the torch power and the argon flow as well as the diameters of tube injector, torch nozzle and the length of reactor are summed up in Table 2.

The study of the CFC-12 decomposition requires the temperature  $T_0$  and velocity  $U_0$  of the argon plasma jet at the inlet of reactor (at  $X=0$ ) which must be known under the operating conditions of

the torch. Considering the argon plasma to be an ideal gas,  $T_0$  and  $U_0$  are calculated from the energy balance at the outlet of the nozzle torch [16]

$$P = Q\rho_a C_p(T_0 - T_a) - \frac{1}{2}Q\rho_a(U_0^2 - U_a^2) \quad (1)$$

with

$$U_0 = \frac{T_0}{T_a} U_a \quad (2)$$

and

$$U_a = 4 \frac{Q}{\pi D^2} \quad (3)$$

where  $P$  the net power to generate the plasma jet is,  $Q$  is the argon volumetric flow rate under the ambient temperature ( $T_a = 300K$ ),  $C_p = 520.3 JKg^{-1}K^{-1}$  is the Argon specific heat,  $\rho_a = 1.7838 Kgm^{-3}$  is the argon density at  $T_a$  and  $U_a$  is the velocity of argon plasma under temperature  $T_a$ .

By applying the above equations and the operating conditions of the torch,  $T_0$  and  $U_0$  are determined. Thus,  $T_0 = 8678K$  and  $U_0 = 467 m/s$ .

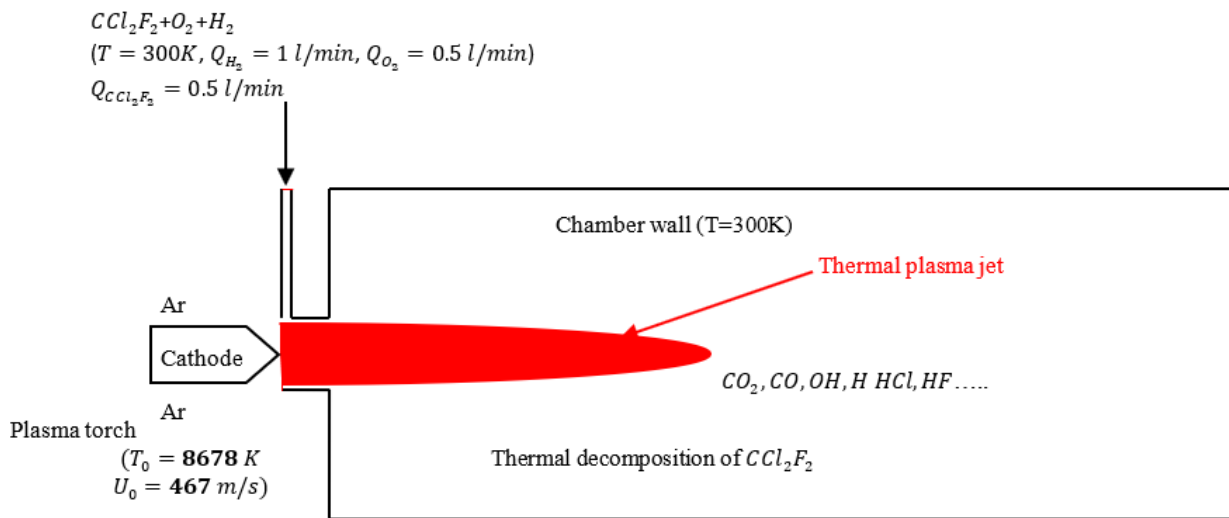


**Fig. 2.** Schematic diagram of plasma reactor

**Table 2**

Working conditions of the plasma reactor illustrated in Figure 2

|                           |                   |
|---------------------------|-------------------|
| Torch diameter, $D$       | 8 (mm)            |
| Injection tube diameter   | 0.5 (mm)          |
| Reaction chamber diameter | 50 (mm)           |
| Reaction chamber length   | 460 (mm)          |
| $Q_{H_2}$                 | 1 (liters/min)    |
| $Q_{O_2}$                 | 0.5 (liters/min)  |
| $Q_{CCl_2F_2}$            | 0.5 (liters/min)  |
| Power, $P$                | 6265.86 (Watt)    |
| Rate argon flow, $Q$      | 47.2 (liters/min) |

## 2.3 Numerical Modeling

The reactive flow is modeled by a set of partial differential equations governing the fluid based on the principle of conservation of mass, momentum and energy with which the kinetic model governing the decomposition of  $\text{CCl}_2\text{F}_2$  with oxygen and hydrogen in argon plasma is associated. These equations take the standard turbulence model CFC-12 into consideration for a two-dimensional plasma flow where an axisymmetric hypothesis is used because of a cylindrical geometry of the reactor.

### 2.3.1 Mathematical formulation

#### 2.3.1.1 Mass conservation and species equations

The mass conservation equation for steady-state reactive flow is given by

$$\frac{\partial \rho u_i}{\partial x_i} = 0 \quad (4)$$

where  $u_i$  is the velocity in the direction  $i$ .

The mass conservation equation for species  $k$  is written as

$$\frac{\partial(\rho(u_i + V_{k,i})Y_k)}{\partial x_i} = \dot{\omega}_k \quad \text{pour } k=1, N \quad (5)$$

where  $V_{k,i}$  the component  $i$  of the diffusion rate  $V_k$  of the species  $k$  and  $\dot{\omega}_k$  is the production rate of the species  $k$ .

Generally, the diffusion rate is given by Fick's law

$$V_{k,i} = -D_k \frac{1}{Y_k} \frac{\partial Y_k}{\partial x_i} \quad \text{pour } k=1, \dots, N_{k-1} \quad (6)$$

#### 2.3.1.2 Momentum equations

The equation of the momentum remains unchanged with the chemical reactions, and it can be written as

$$\frac{\partial \rho u_i u_j}{\partial x_i} = -\frac{\partial P}{\partial x_i} + \frac{\partial \tau_{ij}}{\partial x_i} + \rho \sum_{k=1}^N Y_k f_{k,j} = \frac{\partial \sigma_{ij}}{\partial x_i} + \rho \sum_{k=1}^N Y_k f_{k,j} \quad (7)$$

where  $f_{k,j}$  is the acting volume force on the species  $k$  in the direction  $j$  and  $\tau_{ij}$  is the tensor viscous, given by

$$\tau_{ij} = -\frac{2}{3} \mu \frac{\partial u_k}{\partial x_k} \delta_{ij} + \mu \left( \frac{\partial u_i}{\partial x_j} + \frac{\partial u_j}{\partial x_i} \right) \quad (8)$$

The tensor  $\delta_{ij}$  combines the pressure and the viscous tensor in the following form

$$\delta_{ij} = \tau_{ij} - p \delta_{ij} - \frac{2}{3} \mu \frac{\partial u_k}{\partial x_k} \delta_{ij} + \mu \left( \frac{\partial u_i}{\partial x_j} + \frac{\partial u_j}{\partial x_i} \right) \quad (9)$$

where  $\mu$  is the dynamic viscosity and  $\delta_{ij}$  is the Krönecner symbol.

### 2.3.1.3 Energy conservation equation

It can be written in the sensible enthalpy form

$$\frac{\partial \rho u_i h_s}{\partial x_i} = \dot{\omega}_T + \dot{Q} + \frac{\partial}{\partial x_i} \left( \lambda \frac{\partial T}{\partial x_i} \right) + \tau_{ij} \frac{\partial u_i}{\partial x_j} - \frac{\partial}{\partial x_i} \left( \rho \sum_{k=1}^N V_{k,i} Y_k V_{s,k} \right) \quad (10)$$

The energy flux  $\lambda \frac{\partial T}{\partial x_i}$  is the term of heat diffusion expressed by the Fourier's law.

A second term  $\rho \sum_{k=1}^N V_{k,i} Y_k V_{s,k}$  associates the diffusion of different species with different enthalpies.

The term  $\dot{Q}$  represents a source of heat.

The term  $\dot{\omega}_T$  is the release of heat and is written as

$$\dot{\omega}_T = - \sum_{k=1}^N \Delta h_{f,k}^0 \dot{\omega}_k \quad (11)$$

The set of Navier-Stokes equations for a reactive flow is closed by the equation of state for a perfect gas

$$P = \rho r T \quad (12)$$

## 2.4 Chemical Kinetics

A chemical system (reaction mechanism) of N species that react through L reactions is taken into consideration.

$$\sum_{i=1}^N v'_{i,k} A_i \Leftrightarrow \sum_{i=1}^N v''_{i,k} A_i \quad (13)$$

where  $A_i$  is the chemical symbol of the species,  $v'_{i,k}$  and  $v''_{i,k}$  are the molar stoichiometric coefficients of species  $k$  in reaction  $i$ .

The rate of the whole mass reaction is the total of the rates produced by the L reactions

$$\dot{\omega}_k = \sum_{j=1}^L \omega_{kj} = W_k \sum_{j=1}^L v_{kj} Q_j \quad \text{avec } Q_j = \frac{\dot{\omega}_{kj}}{W_k v_{kj}} \quad (14)$$

where  $v_{kj} = v''_{i,k} - v'_{i,k}$  and  $Q_j$  is the rate of the reaction  $j$  progression which is written as [17]

$$Q_j = K_{ff} \prod_{k=1}^n \left( \frac{\rho Y_k}{M_k} \right)^{v_{ij}^f} - K_{bj} \prod_{k=1}^n \left( \frac{\rho Y_k}{M_k} \right)^{v_{ij}^b} \quad (15)$$

In Eq. (15)  $K_{ff}$  and  $K_{bj}$  are the direct and inverse rates of reaction  $j$ .  $\frac{\rho Y_k}{M_k}$  is the molar concentration of species  $k$ . These rates are a central problem in modeling. They are always modeled using Arrhenius's empirical law.

$$K_{ff} = A_{ff} T^{B_j} \exp \left( - \frac{E_j}{RT} \right) \quad (16)$$

Knowing the individual rate of progression  $Q_j$  of each reaction requires the constant  $A_{fj}$ , the exponent of the temperature  $B_j$ , and the activation energy to be known.

In this study, 17 chemical species and 21 chemical reactions are taken into account by the kinetic model governing the decomposition mechanism of  $\text{CCl}_2\text{F}_2$ , with oxygen and hydrogen in the argon plasma. The main species involved in this work were determined based on a thermodynamic study of the Ar/C/Cl/F/O/H system.

Ar, Cl, O, H,  $\text{O}_2$ , CO,  $\text{CO}_2$ ,  $\text{H}_2$ , OH,  $\text{H}_2\text{O}$ ,  $\text{Cl}_2$ , HCl, HF,  $\text{CCl}_2\text{F}_2$ ,  $\text{CClF}_2$ , F and  $\text{CF}_2$ . In Table 3, the 21 reactions are listed with their direct rates of Arrhenius's empirical law [13].

**Table 3**

Mechanism reactions involved in  $\text{CCl}_2\text{F}_2$  decomposition with  $\text{O}_2$  and  $\text{H}_2$  in argon thermal plasmas.  $A_{fj}$  rate constant  $K_{ff}$  of each forward reaction is expressed by  $K_{ff} = A_{fj} T^{B_j} \exp\left(-\frac{E_j}{RT}\right)$ , where units are given by kilocalories for  $E_j$ , Kelvin for T, and  $R = 1.99 \times 10^{-3}$  kcal/mol/ K

|    | Reactions  | $A_{fj}$  | $B_j$  | $E_j$  | ref     |
|----|--|-----------|--------|--------|---------|
| R1 | $\text{O} + \text{O} + \text{M} = \text{O}_2 + \text{M}$                   | 1.200E+17 | -1.000 | 0.     | [18]    |
| R2 | $\text{O} + \text{CO} + \text{M} = \text{CO}_2 + \text{M}$                 | 6.020E+14 | 0.000  | 3000.  | [18]    |
| R3 | $\text{O}_2 + \text{CO} = \text{O} + \text{CO}_2$                          | 2.500E+12 | 0.000  | 47800. | [18]    |
| R4 | $\text{H} + \text{O}_2 = \text{O} + \text{OH}$                             | 8.300E+13 | 0.000  | 14413. | [18]    |
| R5 | $\text{O} + \text{H}_2 = \text{H} + \text{OH}$                             | 5.000E+04 | 2.670  | 6290.  | [18]    |
| R6 | $\text{OH} + \text{H}_2 = \text{H} + \text{H}_2\text{O}$                   | 2.160E+08 | 1.510  | 3430.  | [18]    |
| R7 | $\text{OH} + \text{OH} = \text{O} + \text{H}_2\text{O}$                    | 3.570E+04 | 2.400  | -2110. | [18]    |
| R8 | $\text{H} + \text{H} + \text{M} = \text{H}_2 + \text{M}$                   | 1.000E+18 | -1.000 | 0.     | [18]    |
| R9 | $\text{H} + \text{OH} + \text{M} = \text{H}_2\text{O} + \text{M}$          | 2.200E+22 | -2.000 | 0.     | [18]    |
| R1 | $\text{OH} + \text{CO} = \text{H} + \text{CO}_2$                           | 4.760E+07 | 1.228  | 70.    | [18]    |
| 0  |  |           |        |        |         |
| R1 | $\text{H} + \text{Cl} + \text{M} = \text{HCl} + \text{M}$                  | 5.300E+21 | -2.000 | -2000. | [19]    |
| 1  |  |           |        |        |         |
| R1 | $\text{Cl} + \text{Cl} + \text{M} = \text{Cl}_2 + \text{M}$                | 3.340E+14 | 0.000  | -1800. | [20]    |
| 2  |  |           |        |        |         |
| R1 | $\text{HCl} + \text{H} = \text{H}_2 + \text{Cl}$                           | 1.690E+13 | 0.000  | 4135.  | [21]    |
| 3  |  |           |        |        |         |
| R1 | $\text{HCl} + \text{O} = \text{OH} + \text{Cl}$                            | 5.240E+12 | 0.000  | 6400.  | [20,22] |
| 4  |  |           |        |        |         |
| R1 | $\text{HCl} + \text{OH} = \text{Cl} + \text{H}_2\text{O}$                  | 2.450E+12 | 0.000  | 1100.  | [24,26] |
| 5  |  |           |        |        |         |
| R1 | $\text{Cl}_2 + \text{H} = \text{HCl} + \text{Cl}$                          | 8.590E+13 | 0.000  | 1170.  | [23]    |
| 6  |  |           |        |        |         |
| R1 | $\text{CCl}_2\text{F}_2 + \text{M} = \text{Cl} + \text{CClF}_2 + \text{M}$ | 8.070E+16 | 0.000  | 63060. | [24]    |
| 7  |  |           |        |        |         |
| R1 | $\text{Cl} + \text{CF}_2 + \text{M} = \text{CClF}_2 + \text{M}$            | 3.600E+17 | 0.000  | 0.00.  | [25]    |
| 8  |  |           |        |        |         |
| R1 | $\text{CCl}_2\text{F}_2 + \text{H} = \text{CClF}_2 + \text{HCl}$           | 5.000E+12 | 0.000  | 9510.  | [26]    |
| 9  |  |           |        |        |         |
| R2 | $\text{CF}_2 + \text{Cl}_2 = \text{CCl}_2\text{F}_2$                       | 3.210E+08 | 0.000  | 2113.  | [27]    |
| 0  |  |           |        |        |         |
| R2 | $\text{HCl} + \text{F} = \text{HF} + \text{Cl}$                            | 2.510E+13 | 0.000  | 350.   | [28]    |
| 1  |  |           |        |        |         |

## 2.5 Calculation Condition

The calculation is performed using the FLUENT 14.5 software associating the standard turbulence model (K- $\epsilon$ ). The finite rate / Eddy-dissipation model was retained in its fast chemistry limit. The steady solver was used with the implicit formulation. The SIMPLE algorithm was adopted to solve the pressure–velocity coupling. To obtain the most accurate results possible, a second order upwind scheme was used for pressure, density, momentum, energy and turbulence equations. The sub-relaxation factors for pressure, density, friction force and momentum are respectively 0.3; 0.5; 1; 0.7; as for all species we adopted 0.85. The values of  $K$  and  $\epsilon$  are  $0.0009375 \text{ m}^2/\text{s}^2$  and  $0.134763 \text{ m}^2/\text{s}^3$ .

### 2.5.1 Boundary conditions and computational domain

Based on the fore mentioned working conditions as shown in Figure 2, the temperature and velocity of the argon plasma at the inlet reactor are respectively 8674 K and 467 m/s, the reactive gas mixture consisting of CFC-12,  $\text{O}_2$  and  $\text{H}_2$  is injected at 2 m/s under ambient temperature (300 K) and the mass fraction of gas mixture (argon and reactive gas mixture) is 0.84 for argon, 0.08 for  $\text{H}_2$  and 0.04 for both CFC-12 and oxygen  $\text{O}_2$ .

The computational domain used in this work is described in Figure 3. In order to obtain accurate results, the residue from all equations (continuity, energy, and the two momentum equations) is less than  $10^{-6}$  and a numerical solution was carried out using the finer volume mesh.

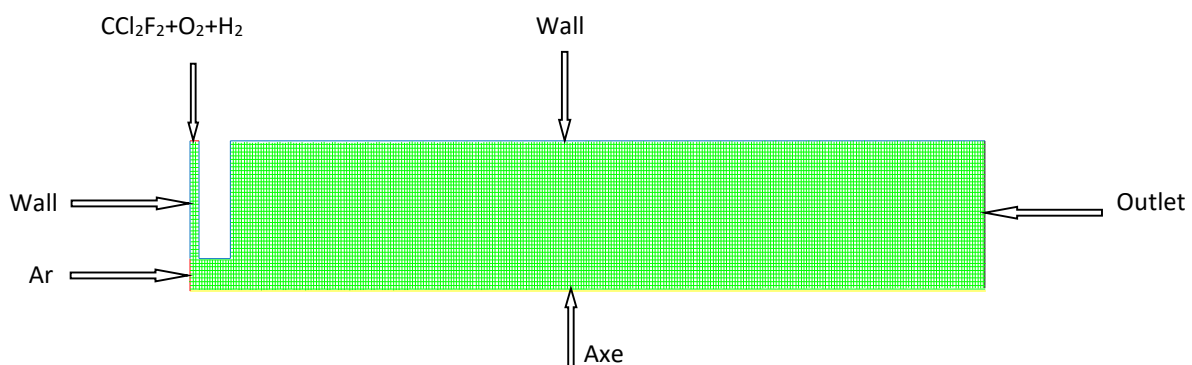
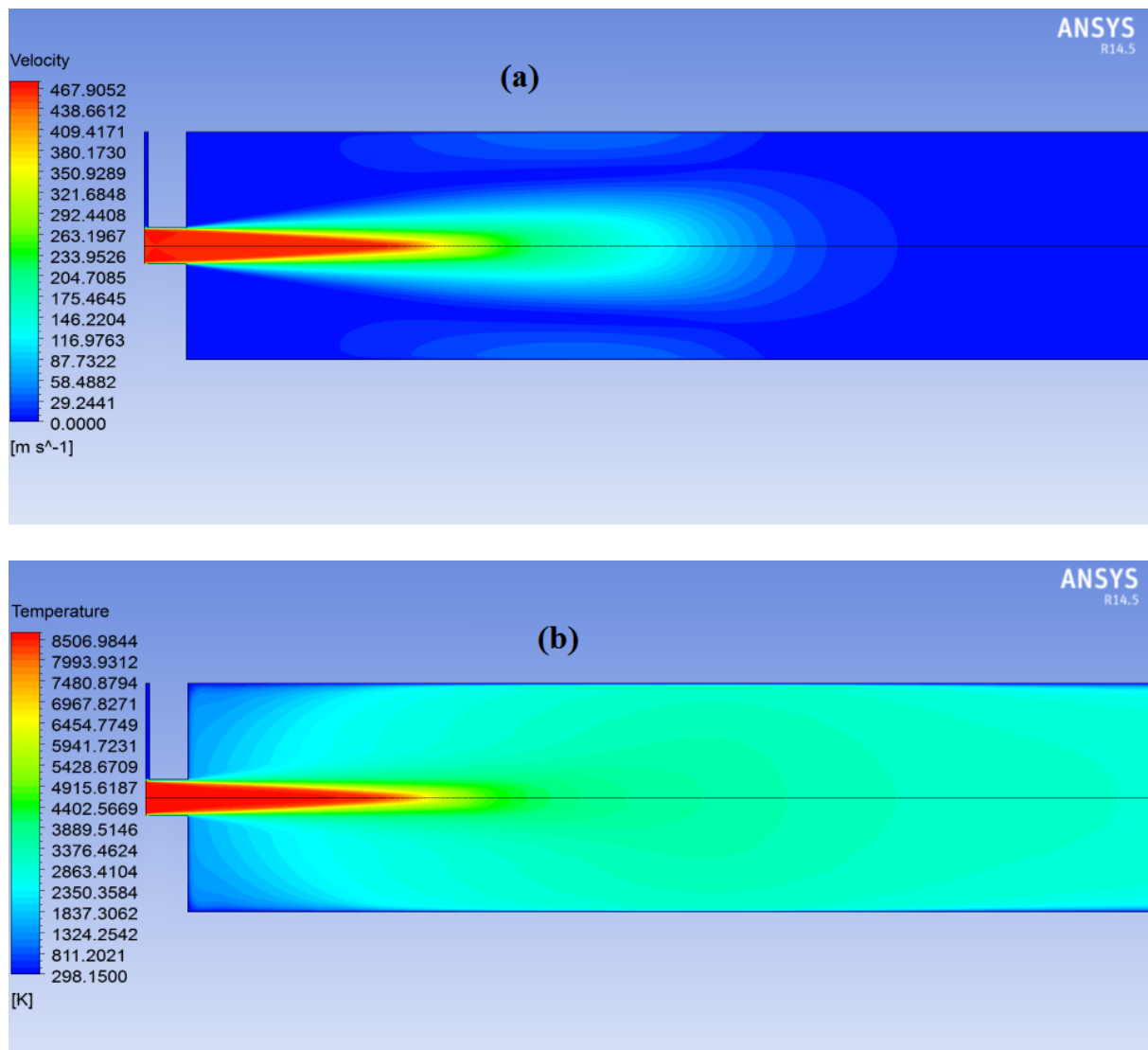


Fig. 3. 2D view of the calculation domain (Mesh) and boundary conditions

## 3. Results and Discussions

As the temperature and velocity of the thermal plasma are very important parameters in the process of CFC-12 decomposition, the contour plot of both temperature and velocity of the reactive flow along the reactor is shown in the Figure 4. The examination of this figure shows that the temperature and the velocity of the jet at the outlet of the torch nozzle are not affected by the radial injection of the gaseous reactants (CFC-12,  $\text{O}_2$  and  $\text{H}_2$ ) because the velocity and the temperature injection (2m/s and 300K) are very small compared to those of the plasma jet at the outlet nozzle (467m/s and 8678K).





**Fig. 4.** Plasma temperature and flow patterns developed in plasma reactor; (a) iso-contours of streamlines and (b) the plasma temperature

As the flow moves away from the nozzle, the jet spreads out in the reactor and the boundary layer phenomena manifest itself at the reactor wall, thus promoting a zone of recirculation of the flow after 25cm. Beyond this zone the temperature and velocity gradients in the radial direction of the reactor decrease and the flow tends to become homogeneous. The axial profile of temperature and velocity along the centerline of the reactor is shown in Figure 5 which indicates the presence of three regions, the heart region ( $0 < x < 10\text{cm}$ ) where both temperature and velocity ( $T_0$  and  $U_0$ ) are represented by a flat profile, followed by the developed region whose main characteristic is the rapid drop in temperature and velocity along the jet ( $10 < x < 28\text{cm}$ ), and the third region in which the temperature and velocity stabilize again. These temperature profiles are in agreement with the work [5, 29] performed on the argon atmospheric thermal plasma jet.

The description of the decomposition of Freon12 is shown in Figure 6 where the  $\text{CCl}_2\text{F}_2$  completely and immediately decomposes as soon as it is injected. This phenomenon results from the high temperature of the plasma argon. The injected gaseous reactants ( $\text{CCl}_2\text{F}_2$ ,  $\text{O}_2$  and  $\text{H}_2$ ) are mainly decomposed into stable species  $\text{CO}_2$ ,  $\text{CO}$ ,  $\text{HCl}$ ,  $\text{HF}$  and  $\text{H}_2\text{O}$ . This result is in agreement with both the thermodynamic investigation and the experimental results obtained by [13].

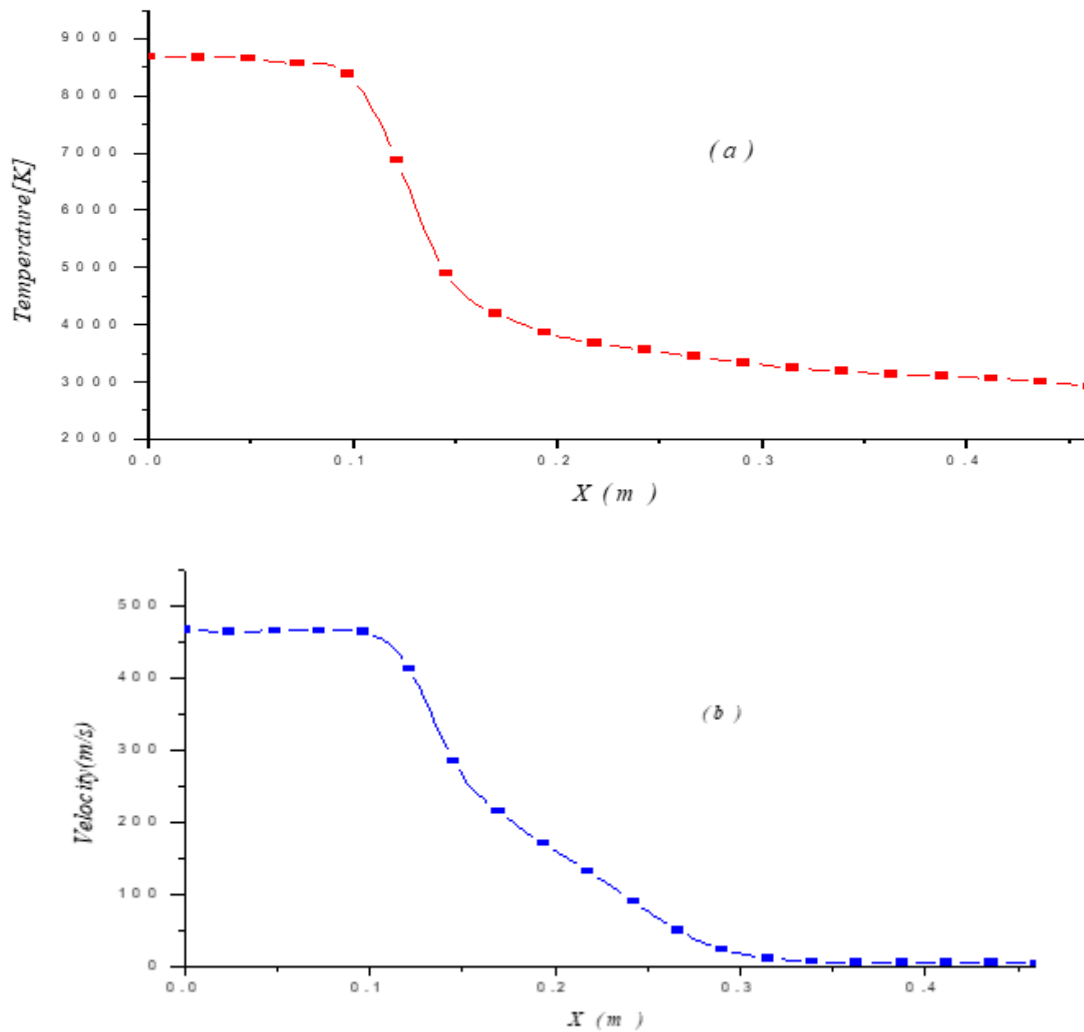


Fig. 5. Calculated axial profile along the centerline of plasma temperature (a) and (b) velocity

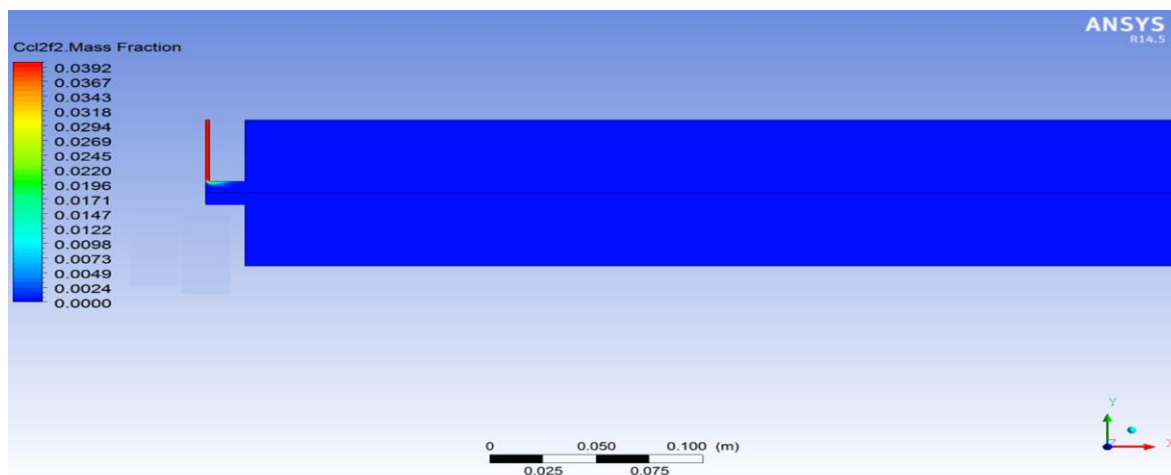
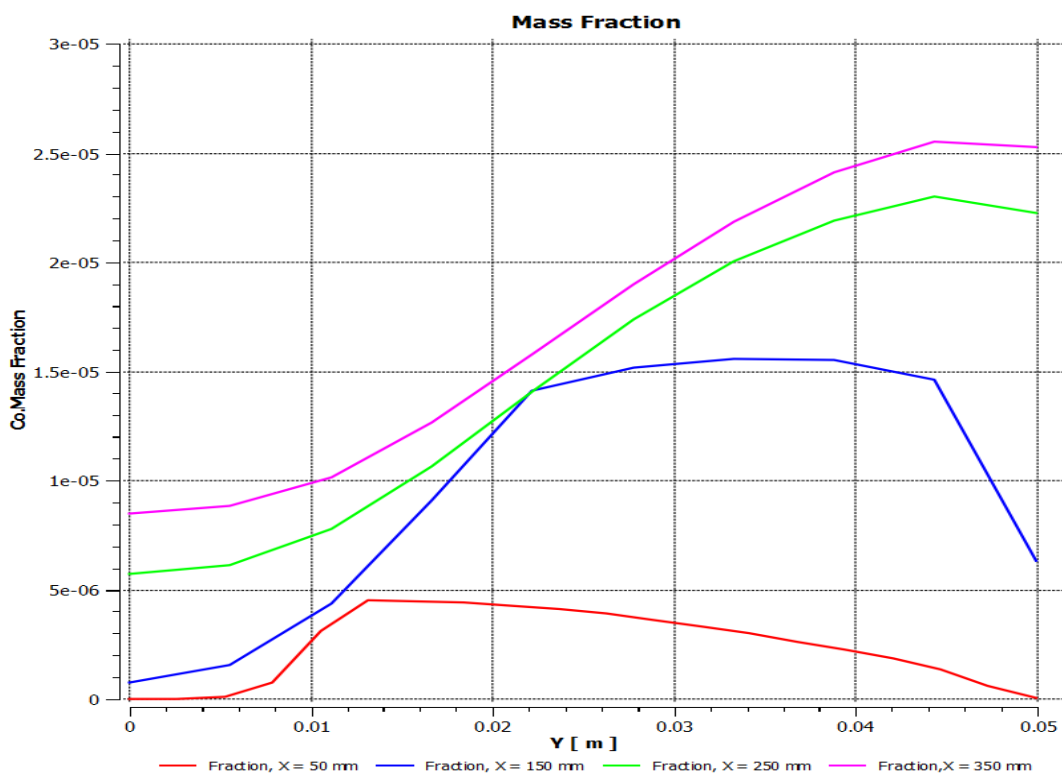
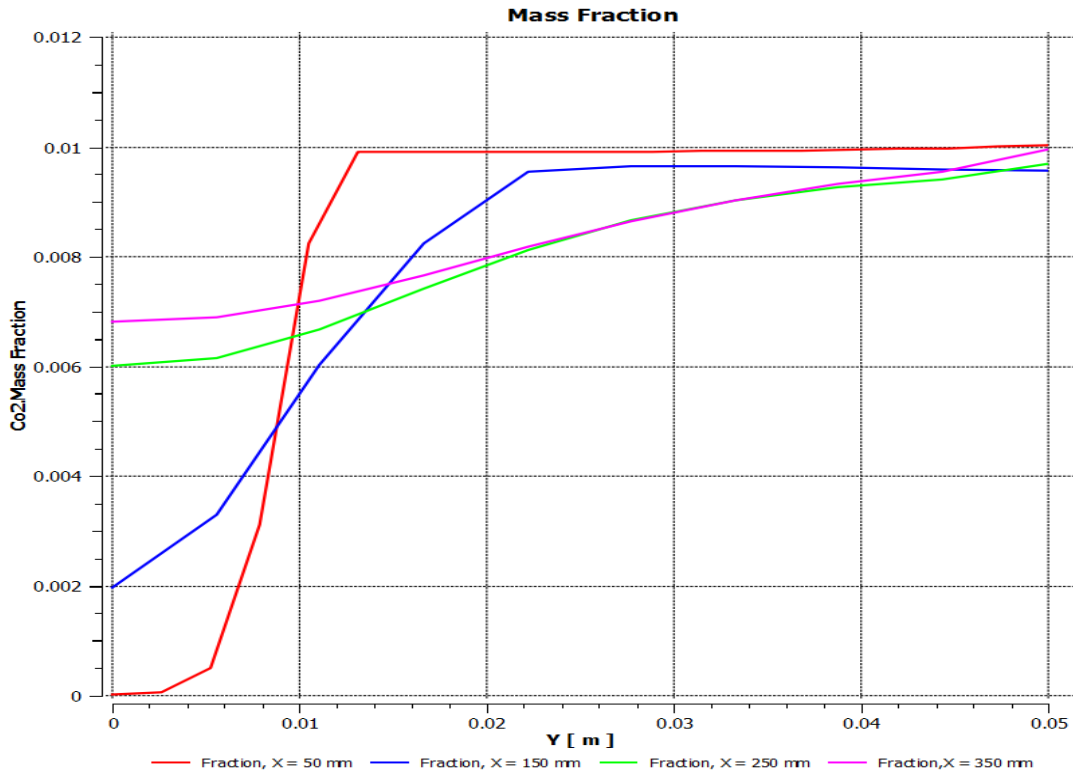
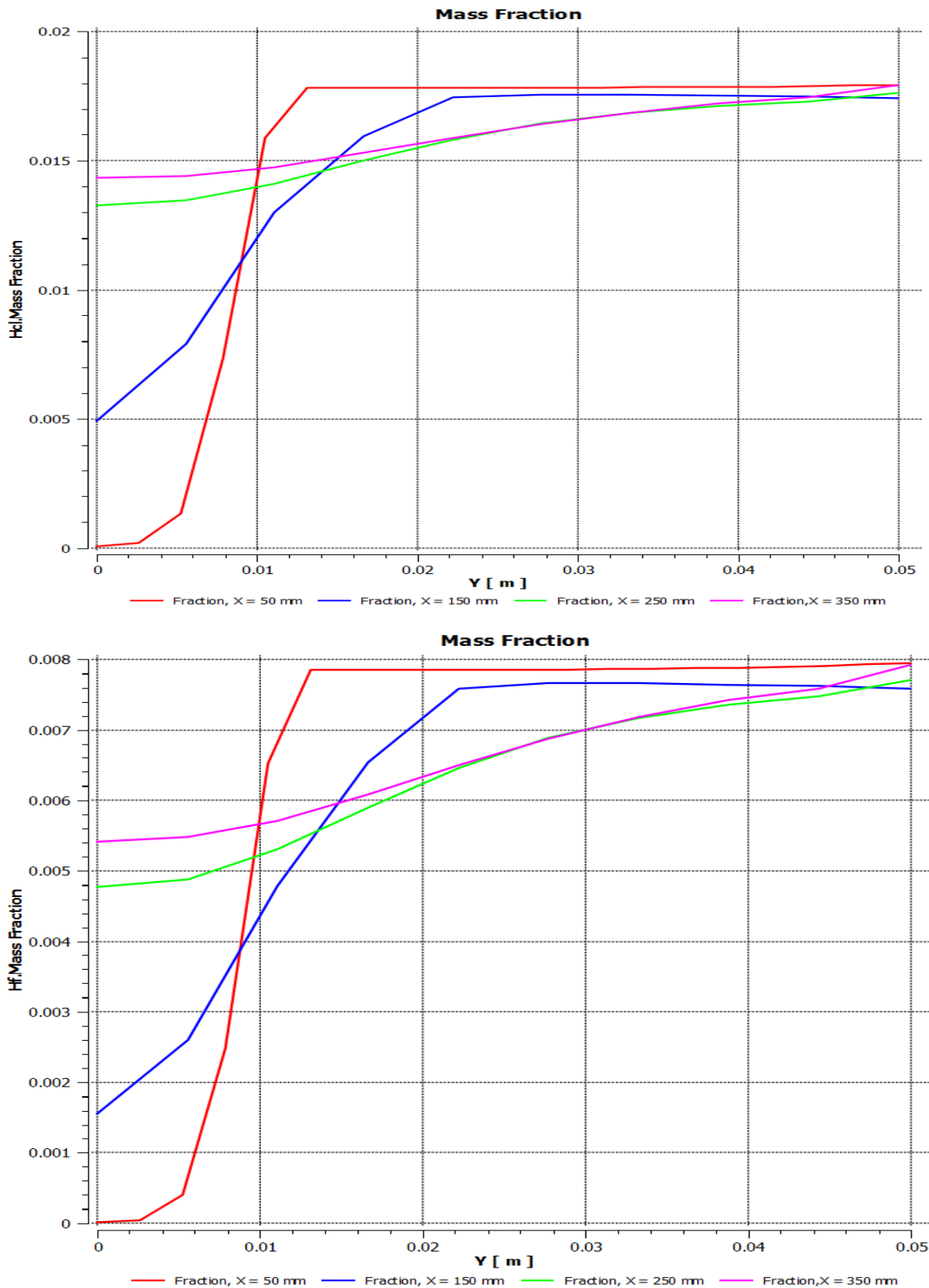


Fig. 6. Calculated mass fractions of CCl<sub>2</sub>F<sub>2</sub>

However, it is worth noting that areas characterized by high temperature (heart and the developed region close to the nozzle) do not allow the formation of these species because the high temperature leads to the formation of atoms and radicals which all combine to form stable chemical species in the cold parts of the reactor (close to the wall and at the outlet of the reactor). This trend

is confirmed by the results of the simulation shown in Figure 7 and 8. Figure 7 illustrates the radial variation in the mass fractions of these molecules resulting from the decomposition of CFC-12 at different axial locations along the reactor respectively  $X = 50$ ,  $X = 150$ ,  $X = 250$  and  $X = 350$  mm. Moreover, the same figure shows that the mass fractions of these chemical species increases with the distance  $X$  and the radius  $r$  throughout the reactor resulting in a drop in temperature of the reaction mixture.





**Fig. 7.** Radial profiles of CO<sub>2</sub>, CO, HCl and HF radicals mass fractions at various axial positions (X = 50, 150, 250, 350 mm);

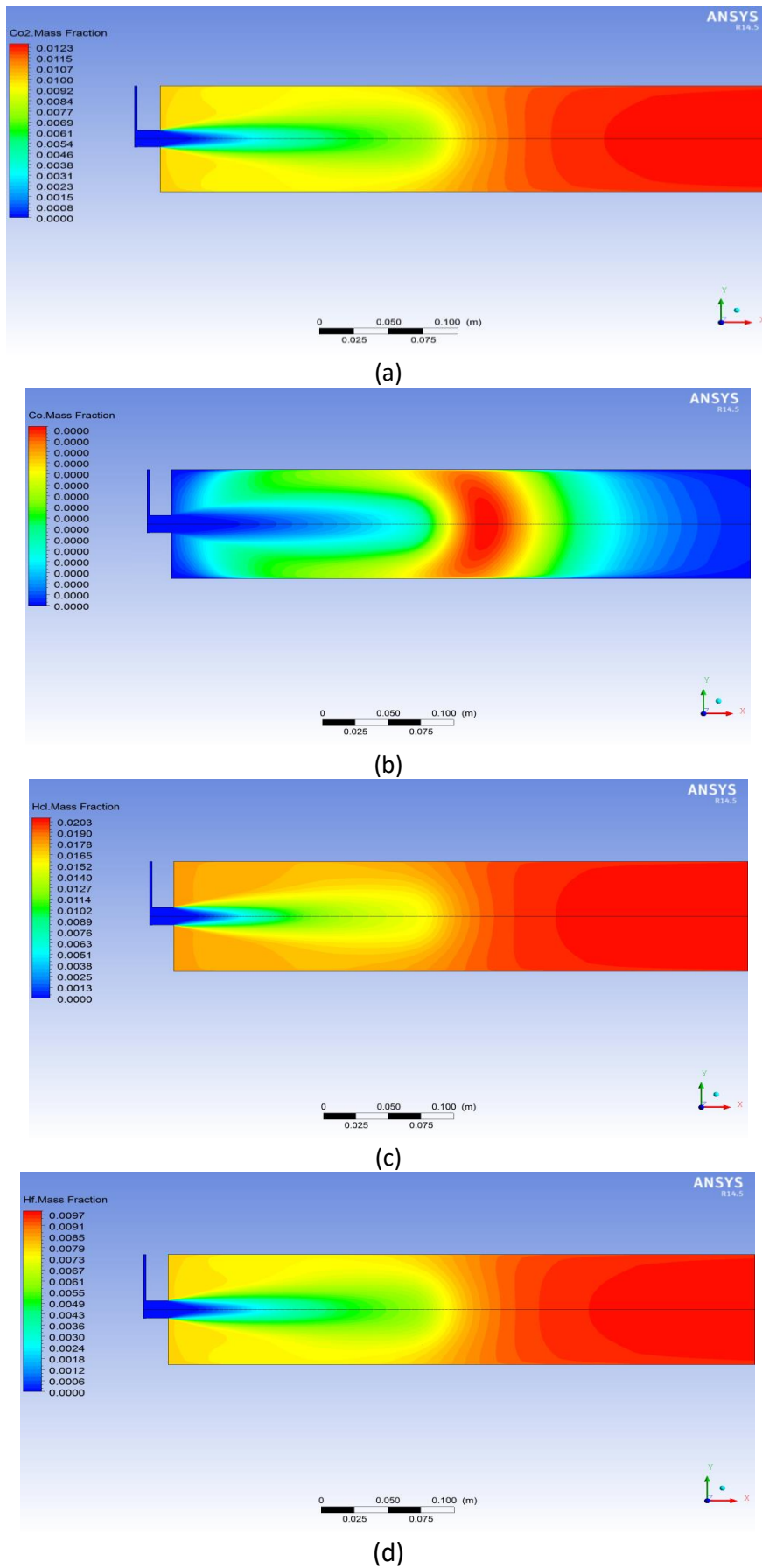


**Fig. 8.** Calculated mass fractions of major reaction products inside a plasma reactor; (a) CO<sub>2</sub>, (b) CO, (c) HCl and (d) HF

While Figure 9 shows the variation in the mass fractions of the dominant species as a result of the reaction ( $\text{CCl}_2\text{F}_2 + \text{O}_2 + \text{H}_2$ ) along the centerline of the reactor. When examining this figure, it can be noticed that the mass fractions of atomic chlorine Cl and hydroxide OH increase until reaching a maximum value corresponding to 15 cm for the atomic chlorine, 13 cm for the hydroxyl. Beyond these distances, the mass fraction decreases to  $10^{-6}$  at 30 cm and 16 cm for atomic chlorine and hydroxide respectively.

On the other hand, the formation of carbon monoxide CO begins at 10 cm and it reaches a maximum value of concentration at 46 cm. As for the carbon dioxide  $\text{CO}_2$ , the gaseous water  $\text{H}_2\text{O}$  and the gaseous hydrogen chloride HCl as well as the hydrogen fluoride HF their mass fractions gradually increase along the centerline until it becomes constant at 20 cm. with the regard to the chlorine  $\text{Cl}_2$ , its evolution is different: because its formation begins from 7.5 cm and then disappears at 12 cm.

As a conclusion of this investigation, the decomposition of CFC-12 with  $\text{O}_2$  and  $\text{H}_2$  in stoichiometric ratio under the operating conditions of the torch plasma mentioned previously, the CFC-12 completely decomposes as soon as it is injected.

In the part of the reactor characterized by a very high temperature (the heart region and developed region close to the torch nozzle), it breaks down into radicals and atoms which combine together in regions characterized by a lower temperature to form stable molecules  $\text{CO}_2$ , HCl, HF and  $\text{H}_2\text{O}$ .

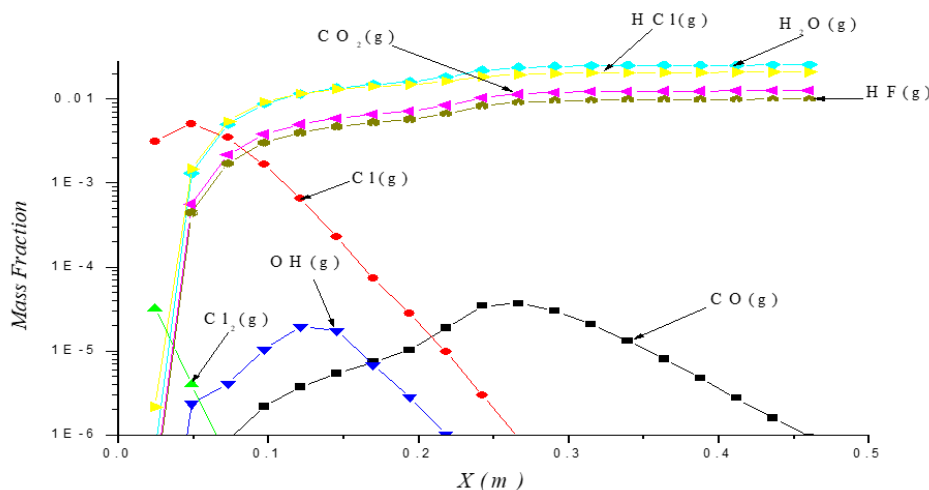


**Fig. 9.** Axial profiles of mass fractions for the main species resulting from the decomposition of  $\text{CCl}_2\text{F}_2$  with  $\text{O}_2$  and  $\text{H}_2$  in stoichiometric ratio

#### 4. Conclusions

CFC-12 decomposition with  $\text{O}_2$  and  $\text{H}_2$  in the argon plasma jet was carried out numerically by CFD software. A set of transport equations combined with chemical kinetics model are solved in two dimensions using (K- $\epsilon$ ) turbulent model to calculate the concentration of main chemical species throughout the plasma reactor resulting from the decomposition process.

A prior thermodynamic investigation was performed on the gas system Ar/Cl/F/O/H between at temperature range from 300K to 6000K in order to determine the dominant species involved when the CFC-12 decomposes.

The results show that the CFC molecule was completely destroyed and it broke down into major species  $\text{CO}_2$ , HCl, HF, and  $\text{H}_2\text{O}$ . The amount of hydrogen in the stoichiometric ratio is sufficient enough to convert Chlorine and fluorine into HCl and HF which makes this process obviously less damaging to the environment because they can be trapped and eliminated by conventional methods.

## Acknowledgement

The authors would like to show their gratitude to Doctor (Brahim Mohammedi), from Birine Nuclear Research Center CRNB, Algeria, for his help and assistance.

## References

- [1] Lu, Q-B. "Cosmic-ray-driven reaction and greenhouse effect of halogenated molecules: culprits for atmospheric ozone depletion and global climate change." *International Journal of Modern Physics B* 27, no. 17 (2013): 1350073.
- [2] Sekiguchi H, Honda T, Kanzawa A *Plasma Chem Plasma Proc* (1993) 13:463
- [3] Lee, Wen-Jhy, Chuh-Yung Chen, Wen-Chang Lin, Ying-Tang Wang, and Ching-Ju Chin. "Phosgene formation from the decomposition of 1, 1-C<sub>2</sub>H<sub>2</sub>Cl<sub>2</sub> contained gas in an RF plasma reactor." *Journal of hazardous Materials* 48, no. 1-3 (1996): 51-67.
- [4] Bosa, Elisabetta, Cristina Paradisi, and Gianfranco Scorrano. "Positive and negative gas-phase ion chemistry of chlorofluorocarbons in air at atmospheric pressure." *Rapid communications in mass spectrometry* 17, no. 1 (2003): 1-8.
- [5] Fauchais, Pierre, and E. Bourdin. "La chimie des plasmas et ses débouchés à court terme sur des synthèses inorganiques à caractère industriel." *Le Journal de Physique Colloques* 38, no. C3 (1977): C3-111.
- [6] M. Jasinski, J. Mizeraczyk, and Z. Zakrewski, *High Temp. Mater. (2002) Proc.* 3, 6.
- [7] Shigeta, Masaya. "Numerical Study of Axial Magnetic Effects on a Turbulent Thermal Plasma Jet for Nanopowder Production Using 3D Time-Dependent Simulation." *Journal of Flow Control, Measurement & Visualization* 6, no. 02 (2018): 107.
- [8] Mostaghimi, Javad, and Maher I. Boulos. "Thermal plasma sources: how well are they adopted to process needs?." *Plasma Chemistry and Plasma Processing* 35, no. 3 (2015): 421-436.
- [9] Shigeta, Masaya. "Modeling and simulation of a turbulent-like thermal plasma jet for nanopowder production." *IEEE Transactions on Electrical and Electronic Engineering* 14, no. 1 (2019): 16-28.
- [10] Chang, J. P., and J. W. Coburn. "Plasma-surface interactions." *Journal of Vacuum Science & Technology A: Vacuum, Surfaces, and Films* 21, no. 5 (2003): S145-S151.
- [11] Van Gompel, Joe. "PFCs in the Semiconductor Industry: A Primer." *Semiconductor International* 23, no. 8 (2000): 321-326.
- [12] Lee, How Ming, and Shiao-Huei Chen. "Thermal Abatement of Perfluorocompounds with plasma torches." *Energy Procedia* 142 (2017): 3637-3643.
- [13] Hidetoshi Sekiguchi Takuya Honda Atsushi Kanzawa. "Thermal Plasma Decomposition of Chlorofluorocarbons." *Plasma Chemistry and Plasma Processing* 13, no.3 (1993): 463-478.
- [14] Ansys, C. F. X. "Solver Theory Guide r12." *ANSYS Inc* (2009).
- [15] White, William B., Selmer Martin Johnson, and George Bernard Dantzig. "Chemical equilibrium in complex mixtures." *The Journal of Chemical Physics* 28, no. 5 (1958): 751-755.
- [16] Snabre, P., M. Announ, J. M. Badie, and B. Granier. "Heat transfer around a spherical particle levitated in argon plasma jet." *The European Physical Journal-Applied Physics* 3, no. 3 (1998): 287-293.
- [17] Kenneth K. KUO, *Principles of combustion*, 2005 2nd ed. John Wiley & Sons ed.
- [18] GRI-Mech v. 1.2 - Frenklach et al. (1995) Report GRI-95/0058.
- [19] Wang, H., T. O. Hahn, C. J. Sung, and Chung King Law. "Detailed oxidation kinetics and flame inhibition effects of chloromethane." *Combustion and flame* 105, no. 3 (1996): 291-307.
- [20] Kerr, J. A. "5. J. Moss teds.), *Handbook of Bimolecular and Termolecular Reactions*, Vol. 1." (1981): 151.
- [21] Adusei, George Yaw, and Arthur Fontijn. "Comparison of the kinetics of O (3P) reactions with the four butenes over wide temperature ranges." *The Journal of Physical Chemistry* 98, no. 14 (1994): 3732-3739.
- [22] Ho, Wen-pin, Robert B. Barat, and Joseph W. Bozzelli. "Thermal reactions of CH<sub>2</sub>Cl<sub>2</sub> in H<sub>2</sub>/O<sub>2</sub> mixtures: implications for chlorine inhibition of CO conversion to CO<sub>2</sub>." *Combustion and Flame* 88, no. 3-4 (1992): 265-295.
- [23] Bozzelli, J.W., Personal Communication (1994).
- [24] Kumaran, S. S., M-C. Su, K. P. Lim, J. V. Michael, A. F. Wagner, L. B. Harding, and D. A. Dixon. "Ab initio calculations and three different applications of unimolecular rate theory for the dissociations of CCl<sub>4</sub>, CFCl<sub>3</sub>, CF<sub>2</sub>Cl<sub>2</sub>, and CF<sub>3</sub>Cl." *The Journal of Physical Chemistry* 100, no. 18 (1996): 7541-7549.
- [25] Codnia, Jorge, and María Laura Azcarate. "Rate measurement of the reaction of CF<sub>2</sub>Cl radicals with O<sub>2</sub>." *Photochemistry and photobiology* 82, no. 3 (2006): 755-762
- [26] Babushok, Valeri I., Gregory T. Linteris, O. C. Meier, and John L. Pagliaro. "Flame inhibition by CF<sub>3</sub>CHCl<sub>2</sub> (HCFC-123)." *Combustion Science and Technology* 186, no. 6 (2014): 792-814.
- [27] Melnikovich, S. V., and F. B. Moin. "Kinetics and mechanism of reaction of difluorocarbene with molecular chlorine." *KINETICS AND CATALYSIS* 27, no. 1 (1986): 17-20.

- 
- [28] Wagner, H. G., Warnatz, J., and Zetsch, C. "Reaction of F atoms with HCl. Ber. Bunsen Ges." 1976.,80, 571–574
- [29] Brossa, M., and E. Pfender. "Probe measurements in thermal plasma jets." *Plasma Chemistry and Plasma Processing* 8, no. 1 (1988): 75-90.